Supporting Information for "The Intersection of Field-Limited Density of States and Matter in Radioluminescence: Nanophotonic Control of Energy Transfer"

Haley W. Jones,[a,b] Yuriy Bandera,[a,b] and Stephen H. Foulger[a,b,c*]

Supporting Text, Figures, and Tables

Radioluminescence of Anthracene

The radioluminescence (RL) spectra of crystalline anthracene powder (99%, Alfa Aesar) is presented in **Figure S1**. Characteristic anthracene radioluminescence is observed with a finger-like peaks spanning ca. 400 nm - 550 nm.

Confirmation of X-ray-induced Förster resonance energy transfer (FRET) between emitters

To confirm Förster resonance energy transfer (FRET) occurs when excited with an X-ray source, the RL spectra of the anthracene, naphthalimide, and rhodamine B derivatives (AMMA, NMMA, and RMMA, respectively) were collected before and after mixing with their respective FRET-pairing emitter. As shown in **Figure S2a**, when the AMMA and NMMA emitters were mixed and excited with an X-ray source, the emission attributed to AMMA decreased by -49% while that of NMMA increased by +42%, indicating X-ray-induced FRET occurs between the AMMA/NMMA FRET pair. As shown in **Figure S2b**, when the AMMA, NMMA, and RMMA emitters were mixed and excited with an X-ray source, the emission attributed to AMMA and NMMA decreased by -63% and -76%, respectively, while that of RMMA increased by +21%, indicating X-ray-induced sequential FRET occurs between the AMMA/NMMA and NMMA/RMMA FRET pairs.

Radioluminescence of the n_1, n_2, and "blank" polystyrene-based nanoparticles

RL spectra of the n_1, n_2, and "blank" polystyrene-based nanoparticles at equivalent concentrations is presented in **Figure S3**. As expected, the n_1 nanoparticles exhibit the greatest emission with very small peaks attributed to AMMA at ca. 405 nm and ca. 425 nm, a larger peak attributed to NMMA centered at 500 nm, and the largest peak attributed to RMMA with a maximum at 620 nm. The n_2 nanoparticles exhibited very small peaks attributed to AMMA at ca. 405 nm and ca. 425 nm, a peak centered at ca. 510 nm, and a peak centered at ca. 640 nm attributed to RMMA and the polystyrene-based host material. Lastly, the "blank" polystyrene-based nanoparticles exhibited a low broad peak centered at ca. 645 nm.

Estimated FRET efficiency between donor/acceptor emitters in n_1 and n_2

Table S1 - S4 presents the estimated FRET efficiency (E_{FRET}) and difference in (ΔE_{FRET}) of each donor/acceptor pair (i.e., AMMA/NMMA and NMMA/RMMA) in n_1 and n_2 when assembled in an OS and the corresponding DS.

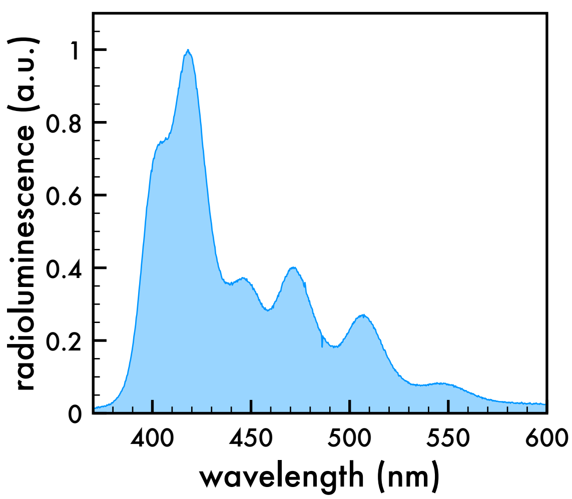

Fig. S1 Radioluminescence spectrum of crystalline anthracene powder.

* foulger@clemson.edu
[a] Center for Optical Materials Science and Engineering Technologies (COMSET), Clemson University, Anderson, SC, 29625
[b] Department of Materials Science and Engineering, Clemson University, Clemson, SC 29634
[c] Department of Bioengineering, Clemson University, Clemson, SC 29634

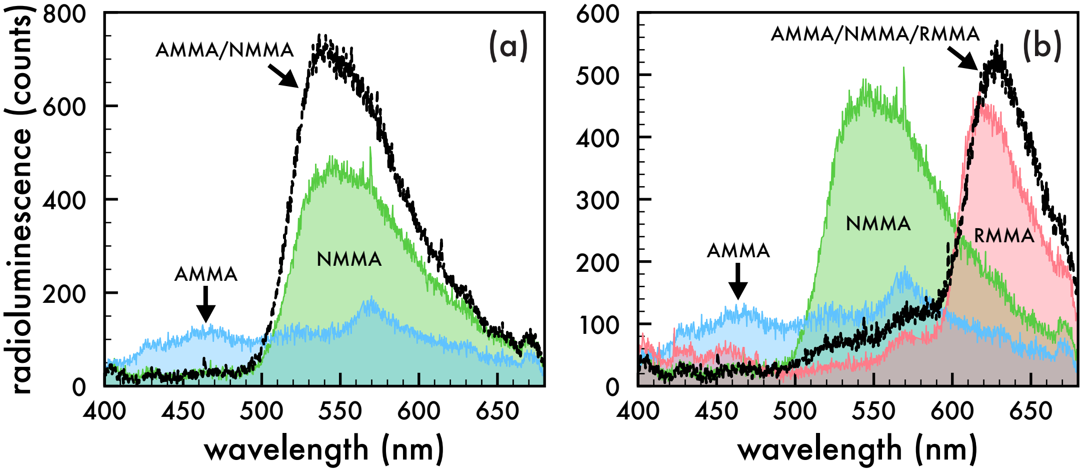

Fig. S2 X-ray-induced Förster resonance energy transfer (FRET) between emitters. (a) Radioluminescence (RL) spectra of AMMA (blue), NMMA (green), and mixed AMMA/NMMA (black dashed line) in 23% (v/v) acetone in deionized water. (b) RL spectra of AMMA (blue), NMMA (green), RMMA (red), and mixed AMMA/NMMA/RMMA (black dashed line) in 23% (v/v) acetone in deionized water. All RL spectra presented in (a,b) was collected at an emitter concentration of 0.77 mg/mL and a 120 second integration time.

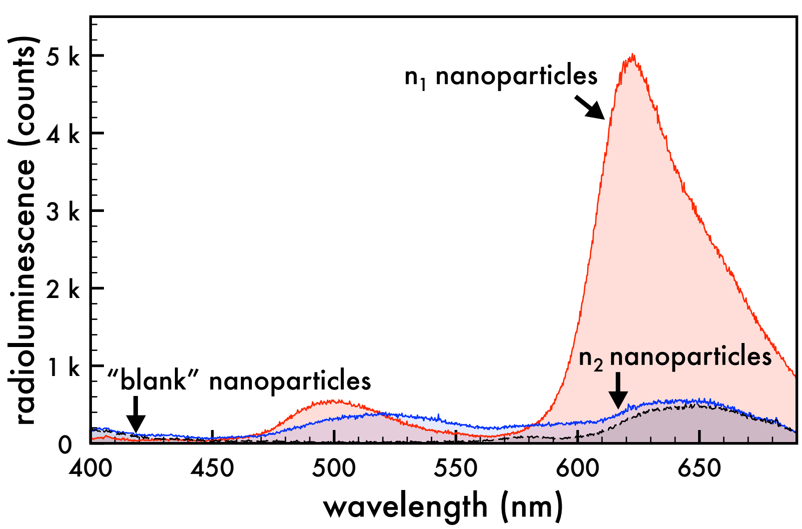

Fig. S3 Radioluminescence of n_1, n_2, and “blank nanoparticles. Radioluminescence (RL) spectra of the n_1 (red), n_2 (blue), and blank (black dashed line) polystyrene-based nanoparticles in deionized water at a concentration of ca. 70 mg/mL (10^{13} particles/mL).

n_1 AMMA/NMMA	λ_{rw} = 441 nm	λ_{rw} = 497 nm	λ_{rw} = 603 nm
OS E_{FRET}	91.3%	75.2%	86.8%
DS E_{FRET}	85.9%	87.2%	86.8%
ΔE_{FRET} (OS - DS)	+5.4%	-12.0%	0.0%

Table S1 Estimated FRET efficiency (E_{FRET}) and difference in E_{FRET} (ΔE_{FRET}) of the AMMA/NMMA donor/ pair in n_1 when assembled in an OS and the corresponding DS.

n_1 NMMA/RMMA	λ_{rw} = 441 nm	λ_{rw} = 497 nm	λ_{rw} = 603 nm
OS E_{FRET}	62.8%	79.5%	42.8%
DS E_{FRET}	65.6%	72.3%	70.4%
ΔE_{FRET} (OS - DS)	-2.8%	+7.2%	-27.5%

Table S2 Estimated FRET efficiency (E_{FRET}) and difference in E_{FRET} (ΔE_{FRET}) of the NMMA/RMMA donor/ pair in n_1 when assembled in an OS and the corresponding DS.

n_2 AMMA/NMMA	λ_{rw} = 424 nm	λ_{rw} = 505 nm	λ_{rw} = 592 nm
OS E_{FRET}	92.5%	78.5%	84.1%
DS E_{FRET}	87.5%	87.9%	85.1%
ΔE_{FRET} (OS - DS)	+5.0%	-9.4%	-1.0%

Table S3 Estimated FRET efficiency (E_{FRET}) and difference in E_{FRET} (ΔE_{FRET}) of the AMMA/NMMA donor/ pair in n_2 when assembled in an OS and the corresponding DS.

n_2 NMMA/RMMA	λ_{rw} = 424 nm	λ_{rw} = 505 nm	λ_{rw} = 592 nm
OS E_{FRET}	33.2%	53.8%	21.2%
DS E_{FRET}	35.8%	47.5%	41.4%
ΔE_{FRET} (OS - DS)	-2.6%	+6.3%	-20.2%

Table S4 Estimated FRET efficiency (E_{FRET}) and difference in E_{FRET} (ΔE_{FRET}) of the NMMA/RMMA donor/ pair in n_2 when assembled in an OS and the corresponding DS.